HNPS Advances in Nuclear Physics

Vol 13 (2004)

HNPS2004

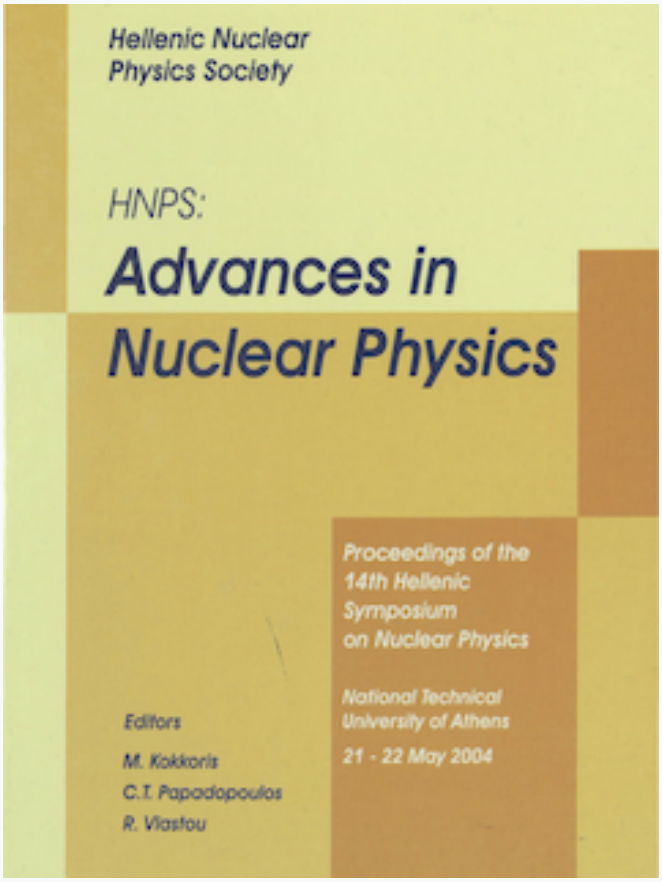

Simulations of Fragment Correlations in the Disintegration of Non-Compact Nuclear Configurations

N. G. Nicolis

doi: 10.12681/hnps.2959

Simulations of Fragment Correlations in the Disintegration of Non-Compact Nuclear Configurations

N.G. Nicolis

Department of Physics, The University of Ioannina, Ioannina 45110, Greece

Abstract

Non-spherical and hollow nuclear configurations have been predicted for intermediate-energy heavy-ion collisions. We have developed a simulation of the emitted heavy fragments in order to establish observables indicative of non-spherical break-up geometries. Starting with a spherical, bubble, spheroidal or a toroidal freeze-out volume configuration, a primary fragment distribution is defined with a given radial collective energy, thermal momentum distribution and intrinsic excitation energy. The outgoing fragments are allowed to propagate along their Coulomb trajectories in a self-consistent manner. Account is taken of the de-excitation of the primary fragments by nucleon and cluster evaporation. Considering 5-fragment partitions, azimuthal distributions and two-fragment correlation functions are constructed and discussed in connection with their associated break-up geometries.

Key words: Low and intermediate-energy heavy-ion reactions; Multifragment emission and correlations

1 Introduction

From the early days of nuclear physics, J.A. Wheeler had suggested the existence of nuclei with non-spherical shapes and investigated the stability of toroidal nuclei [1,2]. About 30 years ago, Siemens and Bethe showed that spherical bubble nuclei with a sufficiently high charge might be stable against a symmetry-preserving breathing deformation [3]. C.Y. Wong has pointed out that the probability of existence of such nuclei should depend on the nuclear temperature [4]. As the nuclear temperature increases the surface tension coefficient decreases and the Coulomb repulsion is pushing nuclear matter outwards, leading to the formation of toroidal and bubble nuclei. L.G. Moretto [5] showed that the depletion of charge in the central cavity of nuclear bubbles

stabilizes them against monopole oscillations. Such objects are however unstable with respect to quadruple and octupole distortions. Generalized rotating liquid drop model calculations show the existence of a potential energy minimum for toroidal shapes even at zero angular momentum, for heavy nuclear systems with masses greater than 300 atomic mass units [6]. Toroidal-shaped configurations have been observed in hydrodynamic collisions [7].

Simulations of nuclear collisions by means of transport equations show the possibility of ring-, disk-, or bubble-shaped nuclear configurations formation in central collisions [8-13]. It was found that different values of the incompressibility of nuclear matter leads to different exotic objects [9].

A number of observables have been suggested as signatures of a noncompact nuclear system configuration breakup, based on the properties of the emitted intermediate mass fragments (IMF's):

a) More IMF's should be generated than would be expected for the decay of a compact configuration at the same temperature [8,14].

b) Some theoretical models predict that the formation of noncompact geometries result in increased cross section for emission of fragments with nearly equal masses with similar charges [12, 15].

c) A non-compact breakup configuration suppresses the sphericity in the emission pattern of heavy fragments [16].

d) Two-body observables, such as angular correlations and relative velocity correlation functions of the IMF's, show some sensitivity in the geometry of the breakup configuration [17].

Experimental evidence for the decay of nuclear matter non-compact geometries up to now is very limited. The article of Stone et al. [16] presents a systematic study of experimental results for the ^{86}Kr + ^{93}Nb system for incident energies ranging from 35 to 95 MeV/nucleon. The authors noticed a 5% enhancement of the intermediate mass fragments emission and a similarity in the fragment charges. They also observe a 5% suppression in the mean value of the sphericity and suppressed flow angles of IMF emission. These observations indicate the existence of exotic breakup geometries to appear for beam energies between 60 and 75 MeV/nucleon.

In order to facilitate the analysis of an experiment of our collaboration [18], we present the development of a simulation code for the investigation of two-body observables as a probe of the shape of the breakup configuration.

2 Description of the simulation

In order to simulate Au + Au collisions at 15 MeV/nucleon [18], we developed a Monte-Carlo simulation code, based on the following considerations:

a) *The composite system*: We assume the formation of a composite system with mass and charge consistent with the mass and charges of the projectile and target. The excitation energy (E*) of the composite system is assumed to result from the complete damping of the relative kinetic energy E_{CM}^{rel} of the projectile and target in the center of mass.

b) *The primary fragment partition*: We consider a partition of the composite mass into N_f fragments. We randomly select the fragments (A_i, Z_i) consistent with the (A,Z) and the neutron deficiency of the composite system.

c) *The excitation energy division*: Assuming that all fragments have the same temperature as the composite system, we assign an excitation energy to each fragment in proportion to its mass.

d) *The freeze-out volume and shape*: The freeze-out volume is constructed by the requirement that its density is one-third of the normal nuclear density. The shape of the freeze-out volume is that of a sphere, a bubble, a spheroid compressed along the beam direction or a torus with its axis along the beam direction. The fragments are assumed spherical, with a normal nuclear density and the assigned excitation energies. They are uniformly distributed in the freeze-out volume and do not overlap. The three-dimensional distributions of fragment centers in the four freeze-out volume configurations are shown in Fig. 1. The spherical configuration has a radius of 11.6 fm. The inner radius of the bubble was taken equal to 3.0 fm. The spheroid configuration was assumed to have an axis ratio of 1.3. The cross section of the toroidal configuration has a radius of 6.5 fm.

e) *The energy balance*: In the center of mass system, the total energy of the entrance channel is $E_{CM}^{rel} + (BE)_p + (BE)_t$, where $(BE)_p$ and $(BE)_t$ are the binding energies of the projectile and target, respectively. E_{CM}^{rel} is the relative kinetic energy of the projectile and target in the center of mass system.

In the freeze-out volume, the total energy of the N_f fragments before evolution is

$$E_{t,kin} + \sum_{i=1}^{N_f} (BE)_i + \sum_{i=1}^{N_f} E_i^* + V_C$$

where $E_{t,kin}$ is the total available kinetic energy of the fragments and V_C is

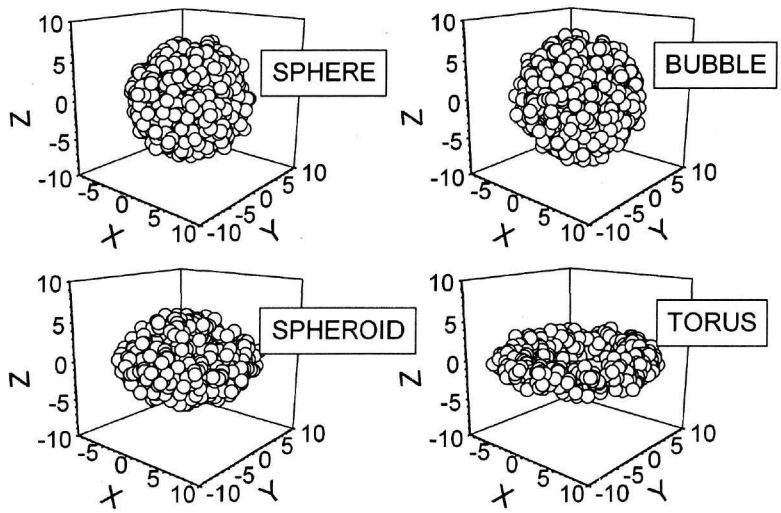

Fig. 1. Three-dimensional distributions of fragment centers in a spherical, bubble, spheroidal and toroidal freeze-out volume configurations. The beam direction is along the z-axis.

the Coulomb interaction energy. From the energy balance, the total available kinetic energy is deduced.

f) *Radial collective flow energy*: The total amount of radial collective energy is estimated from systematics [19], and subtracted from the total available kinetic energy, in order to get the total initial thermal energy (E_{kin}).

g) *Initial momentum and kinetic energy distribution at freeze-out*: It is assumed [20] that at the break-up instant, the fragments are in thermal equilibrium. The total kinetic energy is $E_{kin} = {}^3\!/_2 N_f T$. This condition determines the temperature T. Then, the fragment kinetic energies E_i were selected from a Maxwell-Boltzmann probability distribution function at temperature T

$$\frac{dP(E)}{dE} \propto \sqrt{E} \exp\left(-E/T\right)$$

Momentum directions are chosen randomly in space. In order to conserve momentum, we transform the momentum vectors to a system of zero total momentum. Then, we scale all momenta by a common factor, in order to comply with energy conservation.

h) *Fragment evaporation*: The excited fragments were considered to undergo statistical decay by light particle or cluster emission. The evaporation process

was treated in the Weisskopf approximation, using subroutines from the evaporation code MECO [21]. Angular distributions of the secondary emissions are assumed isotropic. Decay times are extracted from exponential distributions consistent with the appropriate decay widths. The decay history of all fragments, including recoil effects, was recorded.

i) *Fragment propagation*: The fragment trajectories were calculated by numerically integrating the equations of motion, taking into account the mutual Coulomb interaction, charge changes and recoil effects due to fragment deexcitation. Coulomb interactions with the emitted light charged particles or clusters, was not considered.

The output consisted of the freeze-out positions, primary and final fragment (A,Z) and the final velocities.

3 Azimuthal correlations

The analysis of Monte-Carlo events was restricted to cases involving five heavy fragments with (A,Z)=(300,150), thus allowing for some undetected mass and charge. In particular, we examined the characteristics of events consisting of five equal fragments with (A,Z)=(60,28) and five unequal fragments with (A,Z) = (20,10), (40,20), (60,30), (80,35) and (100,45).

First, we examine the distribution of relative azimuthal angles between any two fragments, in a collision event. This azimuthal correlation is shown in Fig. 2, for a spherical freeze-out volume. The dashed line shows the correlation in the case where the fragments are allowed to move outwards from their freeze-out positions without taking the Coulomb interactions into account. If we take the Coulomb interactions and evaporation into account, we end up with the solid curve. We realize that the effect of evaporation is to make the correlation smoother and broader, especially at large angles.

Azimuthal correlations of five equal fragments for a spherical, bubble, spheroid and toroidal freeze-out configurations are shown in Fig. 3(a). It is seen that the spherical and bubble configurations look very similar, whereas the spheroid and toroidal configurations can be differentiated from the characteristic shapes of the correlations they produce. The case of unequal fragments for the four freeze-out configurations is shown in Fig. 3(b). Here, we see that all azimuthal correlations are very similar and do not allow us to differentiate between the freeze-out geometries.

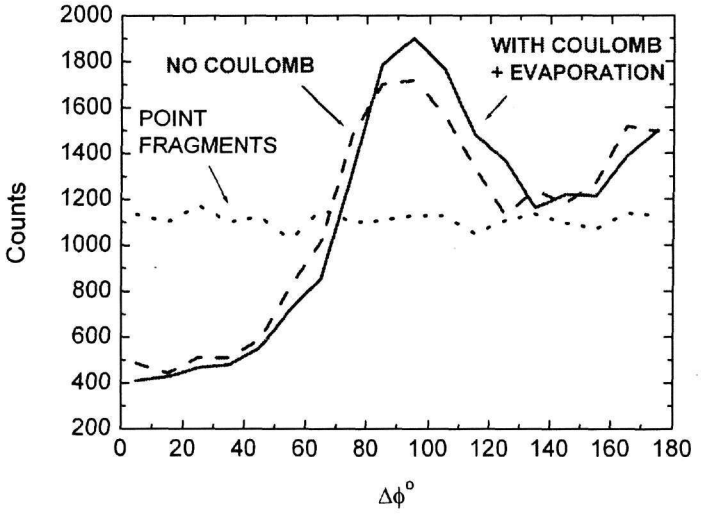

Fig. 2. Azimuthal correlations of five equal fragment events in a spherical freeze-out configuration. The cases of free propagation without Coulomb and with Coulomb plus evaporation effects are shown.

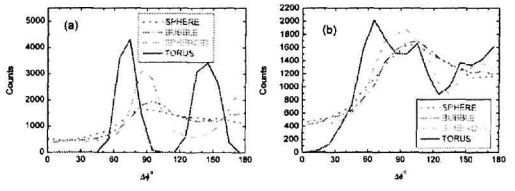

Fig. 3. (a) Azimuthal correlations five equal fragment events for the four freeze-out volume configurations. (b) Same as in (a), for five unequal fragments.

4 Two-body relative velocity correlation functions

The unfavorable case of unequal fragments was further investigated by constructing the two fragment relative velocity correlation functions in the center of mass, defined as

$$1 + R(q) = \frac{\sum Y_{12}(\vec{p}_1, \vec{p}_2)}{\sum Y_1(\vec{p}_1) Y_2(\vec{p}_2)}$$

where $\vec{p}_1$, $\vec{p}_2$ are the fragment momenta, Y_{12} is the coincidence yield of observing one fragment with momentum $\vec{p}_1$ and the other with $\vec{p}_2$, and Y_1, Y_2 are the singles yields. Singles yields were produced with the method of event mixing [22]. The usefulness of this correlation lies in the fact that the relative

velocity distribution, at large relative angles, probes the interaction between all fragments. Therefore, it should be sensitive to the breakup configuration.

For the four freeze-out configurations, the two body relative velocity correlation functions are plotted in Fig. 4 as a function of the reduced velocity v_{red}, which is defined in terms of the relative velocity v_{rel} as $v_{red} = v_{rel}/\sqrt{Z_1 + Z_2}$. This definition of v_{red} eliminates differences between relative velocities due to the fragment charge. As seen in Fig. 4, the four configurations can be easily distinguished in terms of the characteristic shapes of the correlations functions.

Our last result is in agreement with the results of Ref. [17], where it is pointed out that the differences in the fragment correlation functions can be enhanced further by imposing additional gates on transverse and longitudinal components of the relative momentum vector.

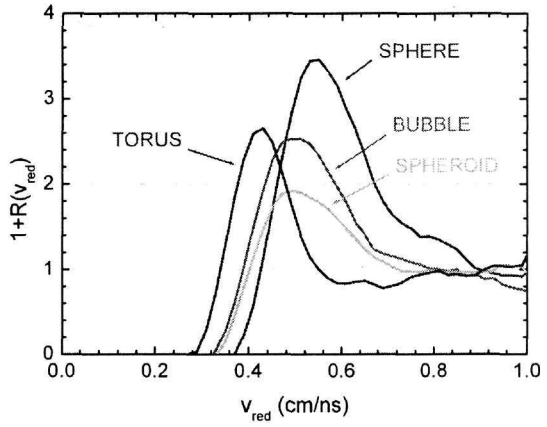

Fig. 4. Two-fragment relative velocity correlation functions, for five unequal fragment events, plotted as a function of the reduced velocity for the indicated freeze-out volume configurations.

5 Summary

We presented preliminary simulations of azimuthal correlations and two-body relative velocity correlation functions of 5-fragment events originating from non-compact breakup configurations, which could be realized in intermediate energy heavy-ion collisions. We considered the breakup of a composite system with (A,Z)=(300,150) from an initial configuration of a compact sphere, a bubble, a spheroid and a torus. The influence of mass (and charge) asymmetry of fragment partitions, initial thermal momentum distribution and evaporation on the azimuthal correlations was examined.

We find that the azimuthal correlations of mass partitions involving similar fragments exhibit patterns indicative of the initial breakup configuration. The azimuthal distributions of asymmetric mass partitions seem to be less sensitive to the breakup geometry. However, even in this unfavorable case, the relative velocity correlation functions could disentangle the breakup geometry.

Under the conditions of a given experimental setup, the above simulations have to be filtered by the response and geometry of the employed setup. Further refinements of the present simulation are also needed. In particular, the role of the initial fragment partitions has to be carefully examined. For this purpose, coupling of our simulations with a statistical multi-fragmentation code is being considered.

References

[1] J.A.Wheeler, "Nucleonic Notebook", 1950 (unpublished).

[2] R.E.Euwema and J.A.Wheeler, unpublished.

[3] P.J.Siemens and H.Bethe, Phys. Rev. Lett. **18** (1967) 704.

[4] C.Y.Wong, Phys. Rev. Lett. **55** (1985)1937.

[5] L.G.Moretto *et al.*, Phys. Rev. Lett. **78** (1997) 824.

[6] C.Fauchard and G.Royer, Nucl. Phys. A**598** (1996) 125.

[7] R. Adams *et al.* Appl. Phys. **39** (1968) 5173.

[8] W.Bauer *et al.*, Phys. Rev. Lett. **69** (1992) 1888.

[9] L.G.Moretto *et al.*, Phys. Rev. Lett. **69** (1992) 1884.

[10] S.R.Souza and C.Ngo, Phys. Rev. C**48** (1993) R2555.

[11] B.Borderie *et al.*, Phys. Lett. B**302** (1993) 15.

[12] H.M.Xu *et al.*, Phys. Rev. C**49** (1994) R1778.

[13] D.O.Handzy *et al.*, Phys. Rev. C**51** (1995) 2237.

[14] L.Phair *et al.*, Phys. Lett. **314** (1993) 271.

[15] C.Y.Wong, Ann.Phys. (N.Y.) **77** (1973) 279.

[16] N.T.B.Stone *et al.*, Phys. Rev. Lett. **78** (1997) 2084.

[17] T.Glasmacher *et al.*, Phys. Lett. B**314** (1993) 265.

[18] R. Paneta, J. Blicharska , J. Brzychczyk, J. Cibor, A. Grzeszczuk, P. Hachaj, S. Kowalski, Z. Majka, N.G. Nicolis, K. Schmidt and W. Zipper for the CHIMERA Collaboration, Proceedings of the *International Workshop on Multifragmentation and Related Topics*, GANIL, Caen, France, November 5-7, 2003.

[19] J. Pochodzalla *et al.*, Preprint GSI 96-31 (1996).

[20] A.S. Botvina *et al.*, Nucl. Phys. A**475**, 663(1987).

[21] N.G. Nicolis, *Proceedings of the 13th Symposium of the Hellenic Nuclear Physics Society*, Ioannina, Greece, May 30-31, 2003. (N.G. Nicolis and T.S. Kosmas Eds.)

[22] M.A. Lisa *et al.*, Phys. Rev. C**44**, 2865(1991).